

3-4-2008

Three-Dimensional Structure of Conotoxin tx3a: A m-1 Branch Peptide of the M-Superfamily

Owen M. McDougal
Boise State University

Matthew W. Turner
Boise State University

Andrew J. Ormond
Boise State University

C. Dale Poulter
University of Utah

Three-Dimensional Structure of Conotoxin tx3a: A m-1 Branch Peptide of the M-Superfamily[†]

Owen M. McDougal^{*,‡}, Matthew W. Turner[‡], Andrew J. Ormond[‡], and C. Dale Poulter[§]

[‡]Department of Chemistry and Biochemistry, Boise State University, Boise, Idaho 83725

[§]Department of Chemistry, University of Utah, Salt Lake City, Utah 84112

*Corresponding author:

Owen M. McDougal
Boise State University
Department of Chemistry and Biochemistry
1910 University Drive, MS 1520
Boise, ID 83725
Phone: 208-426-3964
FAX: 208-426-3027
Email: owenmcdougal@boisestate.edu

[†] This work supported by NIH grants GM 21328, GM 48677, P20 RR016454, and MSTMRI grant # 6PR3381000154.

ABSTRACT

The M-superfamily, one of eight major conotoxin superfamilies found in the venom of the cone snail, contains a Cys framework with disulfide-linked loops labeled 1, 2, and 3 (-CC¹C²C³CC-). M-superfamily conotoxins can be divided into the m-1, -2, -3 and -4 branches, based upon the number of residues located in the third Cys loop between the fourth and fifth Cys residues. Here we provide a three-dimensional solution structure for the m-1 conotoxin tx3a found in the venom of *Conus textile*. The 15 amino acid peptide, CCSWDVCDHPSCTCC, has disulfide bonds between Cys¹ and Cys¹⁴, Cys² and Cys¹², and Cys⁷ and Cys¹⁵ typical of the C1-C5, C2-C4, and C3-C6 connectivity pattern seen in m-1 branch peptides. The tertiary structure of tx3a was determined by 2D ¹H NMR in combination with the combined assignment and dynamics algorithm for nuclear magnetic resonance (NMR) applications CYANA program. Input for structure calculations consisted of 62 inter- and intraproton, 5 phi angle, and 4 hydrogen bond constraints. The root-mean-square deviation values for the 20 final structures are 0.32 +/- 0.07 Å and 0.84 +/- 0.11 Å for the backbone and heavy atoms, respectively. Surprisingly, the structure of tx3a has a “triple-turn” motif seen in the m-2 branch conotoxin mr3a, which is absent in mr3e, the only other member of the m-1 branch of the M-superfamily whose structure is known. Interestingly, injection of tx3a into mice elicits an excitatory response similar to that of the m-2 branch peptide mr3a, even though the conotoxins have different disulfide connectivity patterns.

INTRODUCTION

Cone snails are a class of predatory marine snail, which inject a potent nerve toxin into their prey by way of a disposable hollow tooth. All of the approximately 500 members of the genus *Conus* are venomous hunters of fish, worms, or snails (1). Cone snail venom is typically composed of 40 to 200 small peptides which range in size from 10 to 40 amino acids (2). The great diversity and specificity of *Conus* toxins, termed conotoxins, have been attributed to intense evolutionary pressures. The venom serves as a defense against predators and in some cases, allows the slow moving snail to hunt rapidly moving prey (3).

It is the diversity, specificity and simplicity of conotoxins that contribute to their usefulness as receptor probes. Conotoxins can inhibit or induce muscle contraction in mice, block sodium, potassium or calcium channels, influence glutamate receptor binding, or cause behavioral changes in mice or other animals (4). The specificity shown by individual conotoxins provides the potential to isolate individual receptor types as well as to determine the essential elements for receptor-to-ligand binding (5).

Three-dimensional solution structures of conotoxins determined by NMR spectroscopy have served as models for structure/function relationships. To date, structures for approximately one hundred seven *Conus* peptides have been determined (6). The most studied of these peptides, the α -conotoxins, selectively bind to specific subunits of the nicotinic acetylcholine receptor (nAChR) (7-13). These studies have contributed to an understanding of how nAChRs function and to the development of compounds that specifically target individual receptor types. The α -conotoxins also demonstrate the potential of conotoxins in general to serve as potent and selective probes of closely related receptor types within the human body (14).

Conotoxins of a particular family generally have the same arrangement of cysteine residues in their primary sequence, the same cystine pattern, and cause similar physiological effects in test animals, indicating that they target common receptor types. In contrast, the M-superfamily, which is characterized by the three loop CC-C-C-CC cysteine arrangement, exhibits at least three distinct cystine patterns and a diversity of physiological effects in test animals. The superfamily consists of four branches, m-1, m-2, m-3 and m-4, defined by the number of residues between C4 and C5 (i.e. loop 3) (15). The diversity of peptides exemplified in this superfamily is thought to enhance the cone snail's ability to survive. For example the m-4 branch μ -, ψ -, and κ M-conotoxins with the same disulfide connectivity have a diverse set of molecular targets (Na^+ channel, nicotinic acetylcholine receptor and K^+ channel respectively) (15).

There is considerable structural diversity among the M-superfamily conotoxins. Members of the m-1, m-2, and m-3 branches are smaller (12-19 AA) and contain different disulfide connectivities than those observed for the m-4 branch peptides (22-24 AA). The m-1 branch peptides mr3e and tx3a have C1-C5, C2-C4, and C3-C6 connectivity patterns (16). Other disulfide connectivities within the M-superfamily are C1-C6, C2-C4, C3-C5 for the m-2 branch, and C1-C4, C2-C5, C3-C6 for the m-4 branch (Figure 1). While the receptors targeted by the m-4 branch peptides are well-established, those for the m-1, m-2, and m-3 branch peptides have not been determined. Members of the M-superfamily peptides appear to be very abundant in cone snail venom and presumably are important for survival of the mollusks. The lack of physiological data for m-1, m-2, and m-3 branch peptides has apparently discouraged the widespread pursuit of their three-dimensional structures. Currently structures are only available for the m-1 branch peptide mr3e and the m-2 branch peptide mr3a. No representative structures

have been reported for an m-3 branch peptide (17-18). In contrast, there are several representative structures in the literature for the m-4 branch peptides, whose receptor targets have been determined (19-22).

Figure 1

Interest in tx3a, an m-1 branch conotoxin, arose because members of the M-superfamily appear to be present in every *Conus* species tested to date and the m-1, m-2, and m-3 conotoxins belong to a structurally and pharmacologically distinct group within the M-superfamily that has not been well-characterized. Physiologically tx3a causes hyperactivity in mice upon intracerebral injection at low doses (~2 nmoles), which wears off after only a few minutes, and violent seizures followed by death at high doses (~10 nmoles). The toxin is not active in fish upon intraperitoneal injection. Although the tx3a target receptor is undefined, the observation that it elicits such dramatic effects in mice at nanomolar quantities, yet does not affect fish, indicates that the peptide may be selective for certain receptor types. These physiological effects are similar to those reported for the m-2 conotoxin mr3a (15). We now report the solution structure of conotoxin tx3a, which represents the second example of an m-1 branch peptide of the M-superfamily to be characterized by 2D ^1H NMR.

Materials and Methods

Preparation of tx3a. NMR samples were prepared at a concentration of approximately 4.2 mM in either 100% D₂O (Cambridge Isotope Laboratories, Inc. Andover, MA) or 9:1 (v/v) H₂O/D₂O with 0.01% TFA, pH 4.0. Three successive lyophilizations in D₂O were performed to ensure complete exchange of labile protons. Two-dimensional ^1H NMR experiments and interpretation of spectra were based on established methods (23,24).

NMR Spectroscopy. All NMR data were acquired at 11.75 T on a Varian INOVA 500 MHz NMR spectrometer at 4.0 °C. Proton DQF-COSY (25), NOESY (26), and TOCSY (27) spectra

in D₂O were acquired with the transmitter set to 4.76 ppm and a spectral window of 4500 Hz, giving rise to FID's of 4096 complex points in the ω_2 dimension. Spectra in H₂O were acquired with the transmitter set at 4.8 ppm and a spectral window of 6500 Hz, giving rise to FID's of 4096 complex points in the ω_2 dimension. Transmitter presaturation was applied at the solvent frequency to suppress the H₂O resonance. Series of NOESY spectra were acquired with mixing times of 50, 100, and 200 ms. A TOCSY spectrum was acquired with a mixing time of 200 ms. Spectra were processed on a Silicon Graphics Indigo 2 and/or a Sun Spark 5 workstation using Varian VNMR software.

Restraint Set Generation. The $^3J_{\text{NH}-\alpha}$ values for Cys², Asp⁵, Val⁶, Cys⁷, and Cys¹² were extracted from a high resolution 1D ¹H spectrum. Backbone dihedral phi angle restraints were set to -120 +/- 40° for $^3J_{\text{NH}-\alpha}$ greater than 7.5 Hz and to -65 +/- 25° for a $^3J_{\text{NH}-\alpha}$ less than 5 Hz. Inter- and intraproton distance ranges were derived from NOESY spectra recorded at 4 °C and mixing times of 50, 100, and 200 ms. A plot of cross peak intensity versus mixing time allowed the initial slope of the NOE build-up to be calibrated. As a distance reference, the slope of the build-up for geminal protons was set to 1.8 Å. Restraints were set to 1.8-2.7, 1.8-3.3, and 1.8-5.0 Å for high, medium, and low slopes of NOE intensity plotted against increasing mixing time,

This document is the unedited author's version of a submitted work that was subsequently accepted for publication in Biochemistry, ©2008 American Chemical Society after peer review. To access the final edited and published work see: DOI 10.1021/bi702388b

the times recorded were used for restraints (28).

Structure Calculations. One thousand initial structures generated from random starting conformations were input into the CYANA (V. 2.1) software (29). The distance geometry and gradient minimization calculations were performed to find the conformations which best modeled the 62 upper and 17 lower distance limits, the 5 phi angle, the 4 hydrogen bonds, and the 3 disulfide bonds consistent with the NMR data and the molecular backbone, respectively. A

This document is the unedited author's version of a submitted work that was subsequently accepted for publication in Biochemistry, ©2008 American Chemical Society after peer review. To access the final edited and published work see: DOI 10.1021/bi702388b

pseudo atom correction of 0.5 Å was added to the upper bounds of restraints for methyl and methylene groups. The final set of 20 structures demonstrated an overall root-mean-square deviation among backbone atoms of 0.32 +/- 0.07 Å.

RESULTS

Assignment of Resonances. The complete ¹H resonance assignment for tx3a was achieved using the method of Wüthrich (23) (See Table 1). A combination of DQF-COSY, NOESY, and TOCSY spectra acquired at 4 °C in both 9:1 (v/v) H₂O/D₂O and 100% D₂O were used to eliminate any ambiguities in assignment. Fourteen of the 15 amino acid spin systems for tx3a were identified in the “fingerprint” region of a 200 ms mixing time TOCSY spectrum. The remaining residue, Pro¹⁰, lacks a resonance in this region of the spectrum and was identified later. Ten of the spin systems were confirmed in the “fingerprint” region of a DQF-COSY spectrum and assigned to Cys¹, Cys², Ser³, Asp⁵, Val⁶, Cys⁷, Asp⁸, Ser¹¹, Cys¹² and Thr¹³. Verification of α- and β-proton resonances and the location of the Pro¹⁰ spin system were extracted from TOCSY and DQF-COSY spectra acquired in D₂O. A complete and thorough mapping of all amino acid spin systems was accomplished in this manner.

-Table 1-

The assignment of spin systems to amino acids in the primary sequence of the peptide went as follows. The methyl region between 0.52 and 1.06 ppm in the TOCSY spectrum acquired in 90% H₂O provided information needed to identify Val⁶ and Thr¹³. The two methyl resonances for Val⁶ at 0.55 and 0.52 ppm were easily distinguished from the single methyl in Thr¹³ at 1.06 ppm. Diagnostic resonances were also seen for His⁹, Trp⁴ and Pro¹⁰. The ring protons of His⁹ and Trp⁴ were found in the TOCSY spectrum acquired in D₂O between 6.65 and 9.86 ppm. Trp⁴ was distinguished from His⁹ by the proton on the nitrogen of the Trp⁴ indole

ring. This indole proton, which resonated at 9.86 ppm, is unique to tryptophan. The spin system assigned to Pro¹⁰ originated at 4.13 ppm in the TOCSY spectrum acquired in D₂O. The δ -protons at 3.33 and 3.21 ppm were helpful for assigning resonances for Pro¹⁰ because its α -proton at 4.13 ppm was within 0.04 ppm of the α -protons of Cys², Ser³, Cys⁷ and Asp⁸. A complete trace of the Pro¹⁰ spin system was the only way to distinguish the amino acid from those with overlapping spin systems. The remaining amino acids, Cys¹, Cys², Ser³, Asp⁵, Cys⁷, Asp⁸, Ser¹¹, Cys¹², Cys¹⁴ and Cys¹⁵ all share the same AMX pattern and were sequentially assigned from the 200 ms NOESY spectrum by way of a “NOESY walk”.

Sequential Assignments. The NOESY data were sufficient to observe proton-proton NOE's between the amide proton of one residue and the α -proton of the preceding residue for Cys², Ser³, and Trp⁴, Cys⁷, Asp⁸, and His⁹, and Ser¹¹, Cys¹², and Thr¹³.

Resonance assignments for Val⁶ and Pro¹⁰ came from their unique spin systems as discussed above. The remaining four residues, Cys¹, Asp⁵, Cys¹⁴, and Cys¹⁵, were assigned based on sequential information combined with H β_i to HN $_{i+1}$ cross peaks from the NOESY spectrum. Off-diagonal resonances were observed for the amide and α -protons of Cys² at 8.04 ppm and 4.14 ppm to the β -protons of Cys¹ at 2.62 and 2.26 ppm. Likewise, there was a weak NOE interaction between the amide proton of Cys¹ at 8.09 ppm and the β -protons of Cys¹⁴ at 2.95 and 2.75 ppm that helped to identify Cys¹⁴ and verify the assignment of Cys¹. The assignment of Cys¹⁴ permitted the identification and assignment of Cys¹⁵. There is an NOE between the amide proton of Cys¹⁴ at 8.82 ppm and the β -protons of Cys¹⁵ at 2.14 and 2.01 ppm. Furthermore, there is a cross peak for the NOE between the amide proton of Cys¹⁵ and the β -protons of Cys⁷ at 2.89 and 2.08 ppm. The spin system originating at 7.98 ppm was assigned to Asp⁵ by the process of elimination.

DISCUSSION

Proton Assignments. The small size of conotoxin tx3a made it difficult to observe nuclear Overhauser effects in NOESY spectra acquired at a temperature of 26 °C. A significant improvement in was seen at 4 °C although line widths were significantly broader. The spin systems were easier to resolve at 26 °C due to better spectral resolution and the NOESY spectra were more informative at 4 °C due to slower molecular tumbling. Thus, spectra acquired at both temperatures were used for assignments.

It was immediately apparent from spread of amide resonances that conotoxin tx3a adopted a rigid conformation in solution. In general, random coil peptides have amide proton chemical shifts between 8.09 and 8.45 ppm, while those in conotoxin tx3a were between 7.15 and 8.90 ppm (30). Similarly, the chemical shifts of α -protons in random coils typically range from 4.4 to 4.8 ppm; while those in conotoxin tx3a resonated between 3.94 and 4.94 ppm. Thus, an ordered secondary structure was expected (31-35). The number of constraints per residue and a summary table of all restraints used for structure calculations are provided in Figure 2 and Table 2.

-Figure 2-

-Table 2-

Structure Analysis. The final set of 20 structures for conotoxin tx3a has a mean global backbone rmsd of 0.32 ± 0.07 Å (Figure 3). The backbone of the peptide is well-defined and conserved across all 15 amino acids.

-Figure 3-

The structure of conotoxin tx3a shows a “triple-turn” motif with turns between residues Cys¹ and Asp⁵, Val⁶ and His⁹, and Pro¹⁰ and Thr¹³ (Figure 4). The N-terminal turn between

residues Cys¹ and Asp⁵ is a Type I β turn held in place by a hydrogen bond between the carbonyl of Ser³ and the amide proton of Asp⁵ (distance = 2.23 Å). In β turn nomenclature (36), Cys² and Trp⁴ represent i and $i+2$, respectively. Trp⁴ has its side chain indole ring pointing away from the core of the structure at the kink of the turn. This distinct protrusion significantly defines the surface of the peptide in this region. A second hydrogen bond between the amide proton of Cys¹ and the carbonyl oxygen of Val⁶ further defines the first turn of the molecule. The section of the peptide surrounding Trp⁴ and Asp⁵ constitutes a hydrophilic patch on surface of the molecule. The side chain carboxylate of Asp⁵ and the carbonyl oxygen atoms of Trp⁴ and Asp⁵ point away from the interior of the peptide. This hydrophilic region is further established by “Turn 2.”

The second turn occurs between residues Val⁶ and His⁹. This structural feature is a broad turn constrained by a hydrogen bond between the carbonyl of Cys⁷ and the amide proton of His⁹ (distance = 2.43 Å) and by the disulfide linkage of Cys⁷ and Cys¹⁵. The carboxylate of Asp⁸ is located at the kink in the turn and points away from the interior of the peptide to present a negatively charged region on the surface of the peptide. It deserves comment that the imidazole ring of His⁹ is also oriented away from the interior of the peptide. Thus, there is a region of positive character nearby the negatively charged Asp⁸ carboxylate. The surface created by the second turn of tx3a defines a hydrophilic side of the molecule. Thus, tx3a has a large hydrophilic face on the “Front” and “Side” regions shown in Figure 4. In contrast, the opposite side of the peptide is largely hydrophobic (see the “Back” portion of Figure 4) and corresponds to the location of the methyl and methylene groups of Val⁶, Cys⁷, Cys¹⁴, and Cys¹⁵. The only charged group on the surface of molecule in this region is the C-terminal carboxyl group of Cys¹⁵.

The third turn in the peptide is a Type III β turn between residues Pro¹⁰ and Thr¹³. At the center of this turn is Ser¹¹ ($i+1$). The turn is stabilized by the hydrogen bond between the amide proton of Thr¹³ ($i+3$) and the carbonyl oxygen of Ser¹¹ ($i+1$) (distance = 1.71 Å). This region of the peptide defining the third turn appears significantly less hydrophilic on the surface than the first or second turn regions. Overall, the surface of tx3a is predominantly hydrophilic.

-Figure 4-

Comparison of m-1 branch peptides tx3a to mr3e. Conotoxin tx3a represents the second m-1 branch peptide of the M-superfamily for which a structure is now presented. The structure template for the m-1 branch conotoxins was first described for mr3e (17). The “triple-turn” structure we found for tx3a is substantially different than the “double-turn” motif reported for mr3e despite conserved cystine patterns in the two conotoxins. Differences in the backbone scaffolds of tx3a and mr3e appear to be due to a few key residues. mr3e has two consecutive glycines, Gly⁶ and Gly⁷, that do not appear in the tx3a sequence. These residues permit the sharp bend in turn 1 of the mr3e structure not seen in tx3a (37). Another difference is the number of residues between the cysteine groups. There are 12 residues between C1 and C6 in mr3e and 3 residues between C3 and C4. In contrast, tx3a has 13 residues between C1 and C6 and 4 residues between C3 and C4. Maintaining the same disulfide connectivity while changing the spacing of amino acid residues contributes to the observed structural differences between tx3a and mr3e (Figure 5).

-Figure 5-

tx3a has a more globular shape similar to that of the m-2 branch peptide mr3a, while mr3e has an irregular “flying bird” shape with several amino acid residues jutting out from the peptide backbone (17). The topology of tx3a more closely resembles that of mr3a, although the

surface of tx3a is considerably more hydrophilic. For example, tx3a contains seven polar and charged residues, while mr3a contains only three (Ser⁵, Arg⁹, and Hyp¹⁴). tx3a has a large hydrophilic region consisting of the carboxylate of Asp⁵, the carbonyl oxygen of Cys⁷, the carboxylate of Asp⁸, and the imidazole ring of His⁹ located primarily on the front face of the molecule. In spite of these differences, the two peptides exhibit similar excitatory physiological effects in mice and not toward fish. Thus, the “triple-turn” motif appears to be important for the excitatory behavior seen in mice.

It is well established that m-1, m-2, and m-3 peptides elicit a different symptomatology when injected into mice and fish than do their larger m-4 counterparts. The m-4 branch peptides, consisting of the μ -, ψ -, and κ M toxins, are found primarily in fish-hunting *Conus* species. It is not surprising that the fish hunters require biological warfare agents that rapidly immobilize their fast moving prey. The m-4 peptides are generally paralytic in nature. In contrast, the m-1, m-2, and m-3 peptides are primarily found in the venoms of mollusk and worm-hunting cone snails. The physiological response that these smaller peptides elicit is excitatory. When injected with tx3a, mice become hyperactive in low doses and have seizures resulting in death in higher doses. mr3a is known to cause barrel rolling seizures in mice. There are no reports of activity by m-1, m-2, or m-3 conotoxins in fish. Although experiments have not been conducted with snails or worms, it is possible that exciting a snail or worm prey is advantageous by driving the “feast” from its protective habitat. Although the receptors for these peptides are not known, it is clear that they are active in a distinctive manner from their m-4 counterparts and the topology generated by the “triple-turn” motif seen in tx3a and mr3a is important for their observed activities. The role of the “triple-turn” scaffold in the interaction between tx3a, mr3a, and their target receptors will not be completely understood until their receptors are identified.

ACKNOWLEDGEMENTS

We would like to thank Professor Baldomero M. Olivera, Dr. J. Michael McIntosh, Richard Jacobsen, and Mikal-Anne Waters for assistance and advice on this project, Sean Ruetters for technical support.

REFERENCES

1. Kohn, A. J., Saunders, P. R., Wiener, S. (1960) Preliminary studies on the venom of the marine snail *Conus*, *Annals of the New York Academy of Sciences* 90, 706-725.
2. Myers, R. A., Cruz, L. J., Riviera, J. E., and Olivera, B. M. (1993) *Conus* peptides as chemical probes for receptors and ion channels, *Chem. Rev.* 93, 1923-1936.
3. Olivera, B. M., Rivier, J., Clark, C., Ramilo, C. A., Corpuz, G. P., Abogadie, F. C., Mena, E. E., Woodward, S. R., Hillyard, D. R., Cruz, L. J. (1990) Diversity of *Conus* neuropeptides, *Science* 249, 257-263.
4. Olivera, B. M., Gray, W. R., Zeikus, R., McIntosh, J. M., Varga, J., Rivier, J., de Santos, V., and Cruz, L. J. (1985) Peptide neurotoxins from fish-hunting cone snails, *Science* 230, 1338-1343.
5. Hann, R. M., Pagán, O., and Eterovic, V. A. (1994) The α -conotoxins GI and MI distinguish between the nicotinic acetylcholine receptor agonist sites while SI does not, *Biochemistry* 33, 14058-14063.
6. RCSB Protein Data Base. <http://www.rcsb.org/pdb/advSearch.do>. Search Term: conotoxin (accessed November 2, 2007).
7. Chi, S., Kim, D., Olivera, B. M., McIntosh, J. M., and Han, K. (2004) Solution conformation of α -conotoxin GIC, a novel potent antagonist of α 3 β 2 nicotinic acetylcholine receptors, *Biochem. J.* 380, 347-352.
8. Everhart, D., Cartier, G. E., Malhotra, A., Gomes, A. V., McIntosh, J. M., and Luetje, C. W. (2004) Determinants of potency on α -conotoxin MII, a peptide antagonist of neuronal nicotinic receptors, *Biochemistry* 43, 2732-2737.
9. McIntosh, J. M., Azam, L., Staheli, S., Dowell, C., Lindstrom, J. M., Kuryatov, A., Garrett, J. E., Marks, M. J., and Whiteaker, P. (2004) Analogs of α -conotoxin MII are selective for α 6-containing nicotinic acetylcholine receptors, *Mol. Pharmacol.* 65, 944-952.
10. Loughnan, M. L. and Alewood, P. F. (2004) Physico-chemical characterization and synthesis of neuronally active α -conotoxins, *Eur. J. Biochem.* 271, 2294-2304.
11. Nicke, A., Wonnacott, S., and Lewis, R. J. (2004) α -Conotoxins as tools for the elucidation of structure and function of neuronal nicotinic acetylcholine receptor subtypes, *Eur. J. Biochem.* 271, 2305-2319.
12. Millard, E. L., Daly, N. L., and Craik, D. J. (2004) Structure-activity relationship of α -conotoxins targeting neuronal nicotinic acetylcholine receptors, *Eur. J. Biochem.* 271, 2320-2326.

13. Al-Sabi, A., Lennartz, D., Ferber, M., Gulyas, J., Rivier, J.E., Olivera, B.M., Carlomagno, T. and Terlau, H. (2004) κ M-Conotoxin RIIK, structure and function novelty in a K^+ channel antagonist, *Biochemistry* 43, 8625–8635.
14. Bordia, T., Grady, S. R., McIntosh, J. M., and Quik, M. (2007) Nigrostriatal damage preferentially decreases a subpopulation of $\alpha 6\beta 2$ nAChRs in mouse, monkey, and Parkinson's disease striatum, *Mol. Pharm.* 72, 52-61.
15. Corpuz, G. P., Jacobsen, R. B., Jimenez, E. C., Watkins, M., Walker, C., Colledge, C., Garrett, J. E., McDougal, O., Li, W., Gray, W. R., Hillyard, D. R., Rivier, J., McIntosh, J. M., Cruz, L. J., and Olivera, B. M. (2005) Definition of the M-conotoxin superfamily: characterization of novel peptides from molluscivorous *Conus* venoms, *Biochemistry* 44, 8176-8186.
16. Han, Y., Wang, Q., Jiang, H., Liu, L., Xiao, C., Yuan, D., Shao, X., Dai, Q., Cheng, J., and Chi, C. (2006) Characterization of novel M-superfamily conotoxins with new disulfide linkage, *The FEBS Journal* 273, 4972-4982.
17. Du, W., Han, Y., Huang, F., Li, J., Chi, C., Fang, W. (2007) Solution structure of an m-1 conotoxin with a novel disulfide linkage, *The FEBS Journal* 274, 2596-2602.
18. McDougal, O. M. and Poulter C. D. (2004) Three-dimensional structure of the mini-M conotoxin mr3a, *Biochemistry*, 43, 425-429.
19. Ott, K., Becker, S., Gordon, R. D., and Rüterjans, H. (1991) Solution structure of μ -conotoxin GIIIA analyzed by 2D-NMR and distance geometry calculations, *FEBS Lett.* 278, 160-166.
20. Hill, J.M., Alewood, P.F., and Craik, D.J. (1996) Three-dimensional solution structure of μ -conotoxin GIIIB, a specific blocker of skeletal muscle sodium channels, *Biochemistry* 35, 8824-8835.
21. Van Wagoner, R. M. and Ireland, C. M. (2003) An improved solution structure for ψ -conotoxin PIIIE, *Biochemistry* 42, 6347-6352.
22. Van Wagoner, R. M., Jacobsen, R. B., Olivera, B. M., and Ireland, C. M. (2003) Characterization and three-dimensional structure determination of ψ -conotoxin PIIIF, a novel noncompetitive antagonist of nicotinic acetylcholine receptors, *Biochemistry* 42, 6353-6362.
23. Wüthrich, K. (1986) *NMR of Proteins and Nucleic Acids*, Wiley: New York.
24. Bax, A. (1989) Two-dimensional NMR and protein structure, *Annu. Rev. Biochem.* 58, 223-256.

25. Rance, M., Sørensen, O.W., Bodenhausen, G., Wagner, G., Ernst, R. R., and Wüthrich, K. (1983) Improved spectral resolution in COSY proton NMR spectra of proteins via double quantum filtering, *Biochem. Biophys. Res. Commun.* *117*, 479-485.
26. Jeener, J., Meier, B. H., Bachmann, P., and Ernst, R. R. (1979) Investigation of exchange processes by two-dimensional NMR spectroscopy, *J. Chem. Phys.* *71*, 4546-4553.
27. Braunschweiler, L., and Ernst, R. R. (1983) Coherence transfer by isotropic mixing: application to proton correlation spectroscopy, *J. Magn. Reson.* *53*, 521-528.
28. Keepers, J. W., and James, T. L. (1984) A theoretical study of distance determinations for NMR. Two-dimensional nuclear Overhauser effect spectra, *J. Magn. Reson.* *57*, 404-426.
29. Güntert, P., Mumenthaler, C. & Wüthrich, K. (1997) Torsion angle dynamics for NMR structure calculation with the new program DYANA, *J. Mol. Biol.* *273*, 283-298.
30. Bundi, A., and Wüthrich, K. (1979) Proton NMR parameters of the common amino acid residues measured in aqueous solutions of the linear tetrapeptides H-Gly-Gly-X-L-Ala-OH, *Biopolymers* *18*, 285-297.
31. Wishart, D. S., Sykes, B. D., and Richards, F. M. (1991) Relationship between nuclear magnetic resonance chemical shift and protein secondary structure, *J. Mol. Biol.* *222*, 311-333.
32. Wishart, D. S., Sykes, B. D., and Richards, F. M. (1991) Simple techniques for the quantification of protein secondary structure by proton NMR spectroscopy, *FEBS Lett.* *293*, 72-80.
33. Wishart, D. S., Sykes, B. D., and Richards, F. M. (1992) The chemical shift index: a fast and simple method for the assignment of protein secondary structure through NMR spectroscopy, *Biochemistry* *31*, 1647-1651.
34. Wishart, D. S., Bigam, C. G., Holm, A., Hodges, R. S., and Sykes, B. D. (1995) ^1H , ^{13}C , and ^{15}N random coil NMR chemical shifts of the common amino acids. I. Investigations of nearest-neighbor effects, *J. Biomol. NMR* *5*, 67-81.
35. Volkman, B. F., Nohaile, M. J., Amy, N. K., Kustu, S., and Wemmer, D. E. (1995) Three-dimensional solution structure of the N-terminal receiver domain of NTRC, *Biochemistry* *34*, 1413-1424.
36. Rose, G. D., Gierasch, L. M., and Smith, J. A. (1985) Turns in peptides and proteins, *Adv. Protein Chem.* *37*, 1-109.
37. Voet, D. and Voet, J. G. (2004) *Biochemistry*. United States of America: John Wiley & Sons, Inc. p.222-223.

TABLES

Residue HN		α	β	Other
Cys 1	8.09	4.19	2.62, 2.26	
Cys 2	8.04	4.14	3.34, 3.20	
Ser 3	8.70	4.07	3.66, 3.66	
Trp 4	8.45	3.94	3.09, 2.97	2H 7.10 4H 7.41 5H 6.65 6H 7.00 7H 7.20 NH 9.86
Asp 5	7.98	4.56	2.75, 2.65	
Val 6	7.45	4.30	1.84	γ 0.55, 0.52
Cys 7	7.26	4.17	2.89, 2.08	
Asp 8	8.61	4.10	3.68, 3.68	
His 9	8.37	4.02	3.08, 3.00	2H 7.03 4H 7.12
Pro 10		4.13	2.05, 1.95	γ 1.74, 1.45 δ 3.33, 3.21
Ser 11	7.38	4.26	2.86, 2.51	
Cys 12	7.15	4.50	2.59, 2.32	
Thr 13	8.90	4.04	3.99	γ 1.06
Cys 14	8.82	4.90	2.95, 2.75	
Cys 15	8.88	4.94	2.14, 2.01	

Table 1. Proton resonance assignments for conotoxin tx3a at a temperature of 4 °C.

Distance Restraints		Dihedral Restraints	
Intraresidue	4	Phi angle	5
Sequential	26	Hydrogen bond	4
Medium	22	Total 9	
Long	48		
Total 100			

Table 2: Restraints used to determine the structure of tx3a.

FIGURE LEGENDS

1. A summary of the four branches of the M-Superfamily containing the conserved CC-C-C-CC cysteine pattern with divergent cystine connectivity.
2. A distribution of distance constraints as a function of their residue number used for the structure determination of conotoxin tx3a. The white areas represent intraresidual constraints, light gray areas symbolize sequential constraints, dark gray areas show medium-range NOE's ($d_{ij} \leq 5 \text{ \AA}$) and black areas depict long-range NOE's ($d_{ij} \geq 5 \text{ \AA}$).
3. An overlay of the backbone atoms of tx3a for the final 20 structures generated by CYANA.
4. Three-dimensional structures of tx3a. Shown is the backbone structure identifying each of the turns (top left), turn 1 from Cys¹ to Asp⁵ (green), turn 2 between Val⁶ and His⁹ (red), and turn 3 between Pro¹⁰ and Thr¹³ (blue). The disulfide bonds are shown in yellow with the cystine residues numbered. Also shown are the front, side and back views of the surface of the peptide. Blue regions represent electropositive surfaces, red regions are electronegative surfaces, and white/faintly colored regions are hydrophobic/nonpolar surfaces.
5. Comparison between two m-1 branch peptides, tx3a and mr3e, and m-2 branch peptide, mr3a. Scaffold structures of tx3a, mr3e, and mr3a are labeled A, B, and C, respectively. Frontal surface structures of tx3a (D), mr3e (E), and mr3a (F), showing the "flying bird" depiction of mr3e and the "plucked chicken" representation for tx3a and mr3a. Blue regions represent electropositive surfaces, red regions are electronegative surfaces, and white/faintly colored regions are hydrophobic/nonpolar surfaces.

FIGURES

Figure 1

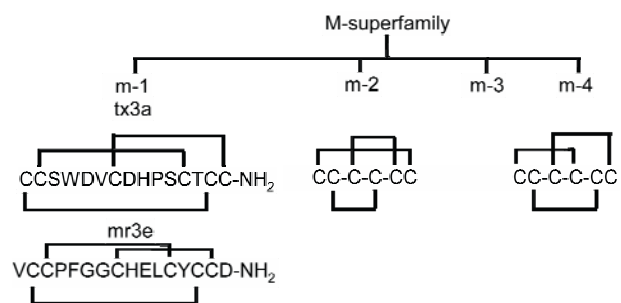


Figure 2

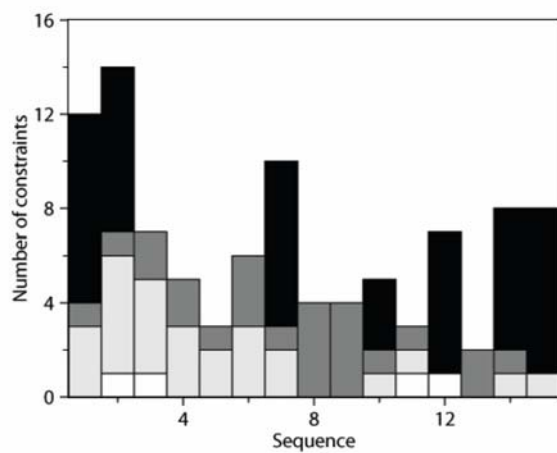


Figure 3

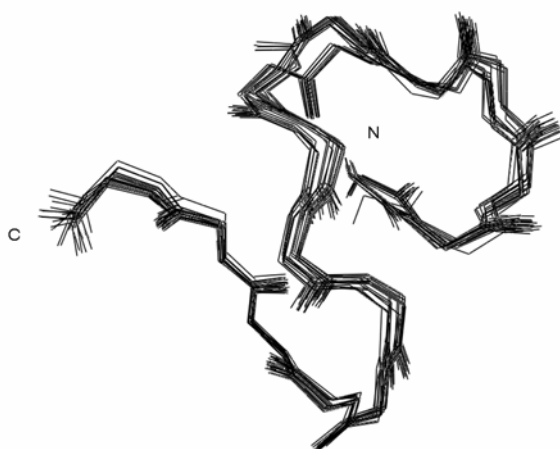


Figure 4

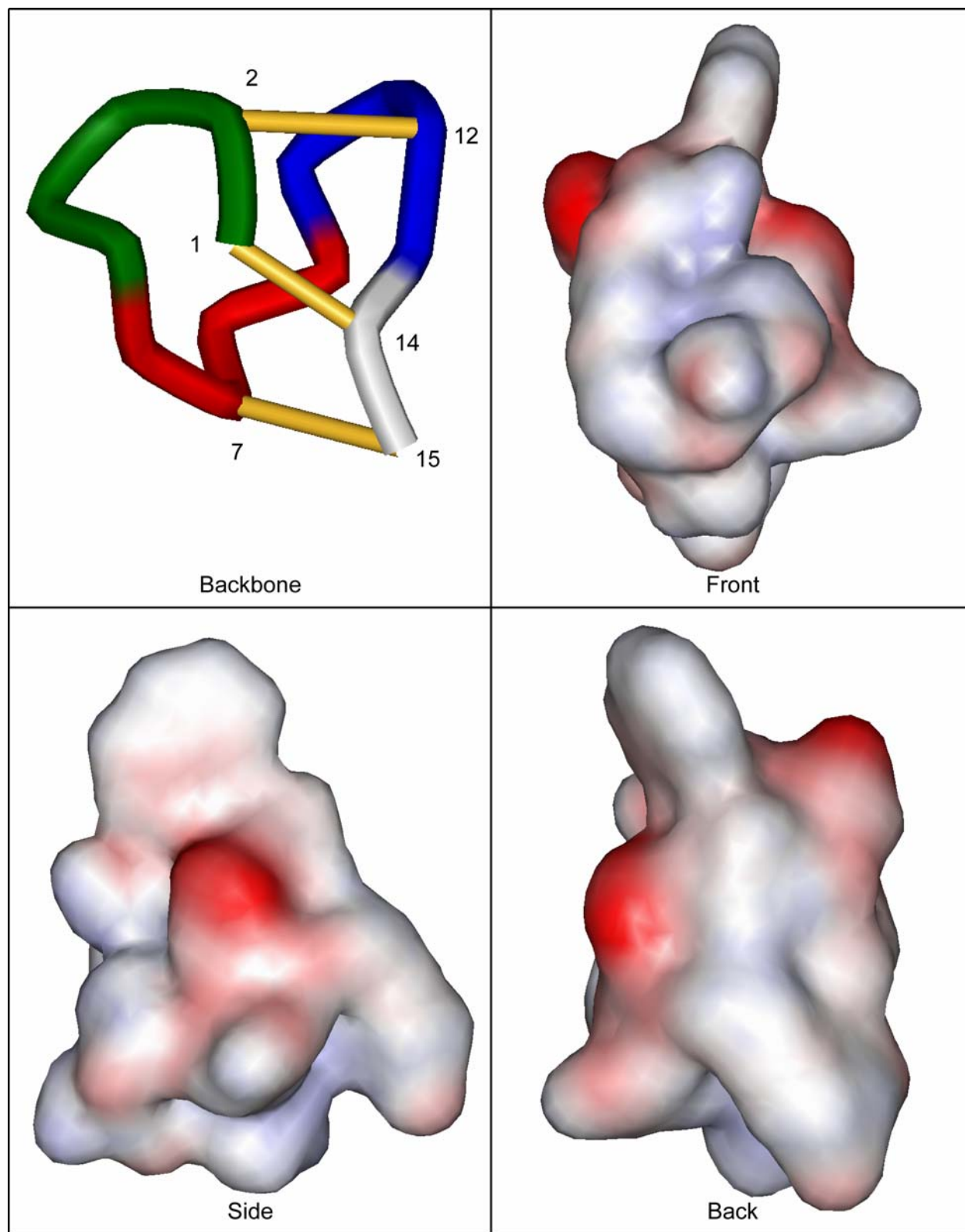
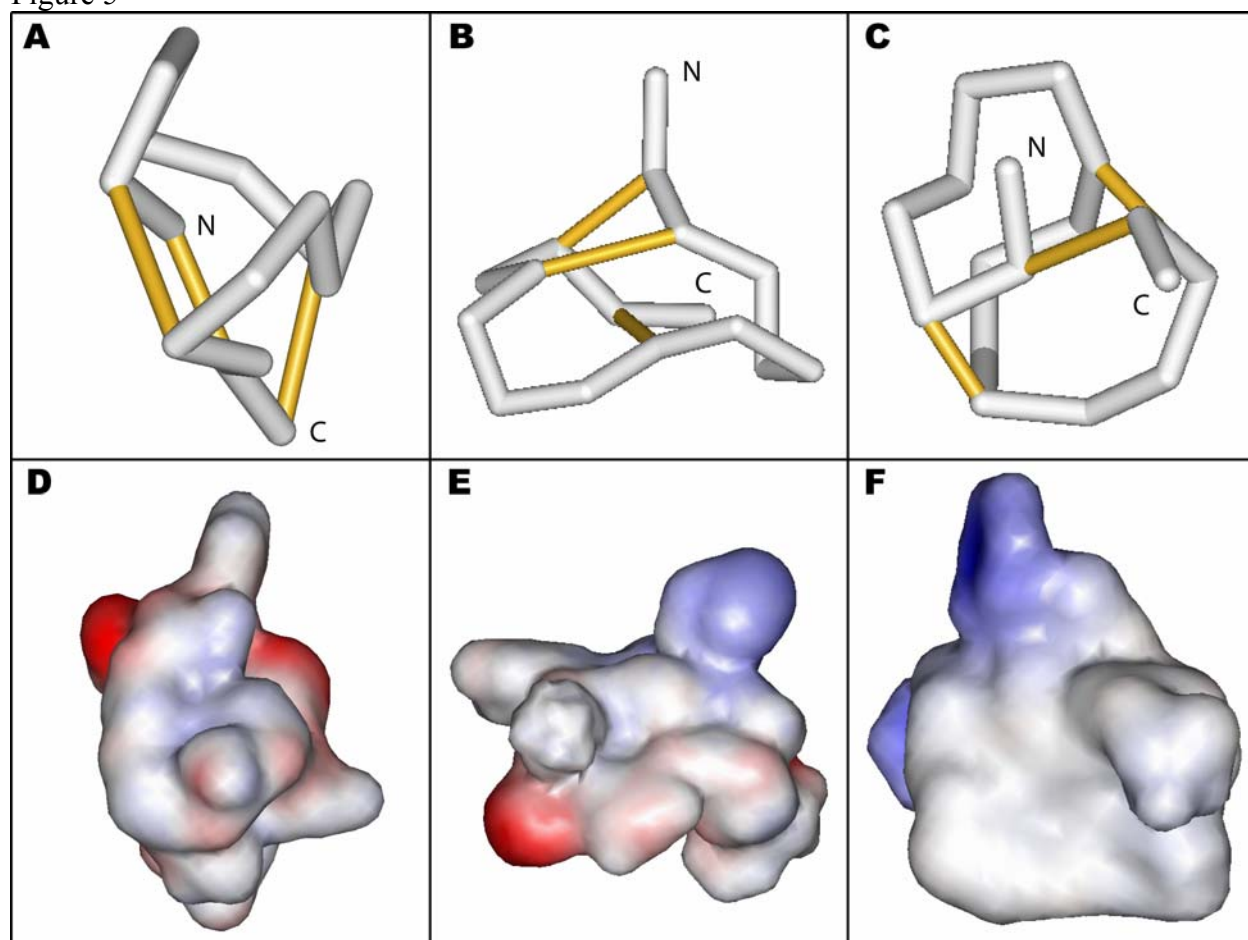


Figure 5



FOR TABLE OF CONTENTS USE ONLY

Three-Dimensional Structure of Conotoxin tx3a: A m-1 Branch Peptide of the M-Superfamily[†]

Owen M. McDougal^{‡*}, Matthew W. Turner[‡], Andrew J. Ormond[‡], and C. Dale Poulter[§]

[‡]Department of Chemistry and Biochemistry, Boise State University, Boise, Idaho 83725

[§]Department of Chemistry, University of Utah, Salt Lake City, Utah 84112

*Corresponding author

